HEAT TRANSFER IN STEADY-PERIODIC FLOWS OVER HEATED MICROWIRES

S. Yesilyurt, M. Ozcan, G. Goktug
Sabanci University, Istanbul, Turkey, 34956

ABSTRACT

Effects of Reynolds number (Re), nondimensional drive frequency (Sr_p) and amplitude of y-oscillations in the flow on the heat transfer coefficient and its frequency response characteristics for oscillatory flows over a micro wire are presented here. Time-averaged Nusselt numbers (Nu) at the stagnation point and averaged over the cylinder are calculated for Re = 10, 30 and 50, $.001 < Sr_p < 1.$, and oscillation amplitudes, V_p, of 0.1 and 0.2 (for Re = 50). We used a formulation that allows decomposition of the flow into mean and periodic components, and used finite-element simulations to solve for the mean flow over the cylinder. Periodic component of the flow contributes to an artificial body force in the Navier-Stokes equation. According to our simulations, time-averaged Nusselt numbers are not strongly affected by oscillations. Largest increase in the time-averaged average Nu is only 3% larger than its unforced value. Nusselt oscillations have multiple modes and we used Fourier Transform to identify each mode and calculate its corresponding amplitude. The mode for which the frequency is twice as much as the driving frequency is the dominant mode for Sr_p up to 0.1 for all Reynolds numbers studied here. For larger drive frequencies, the second mode dies off; for Re = 30 and 50 amplitude of the first mode at the drive frequency takes over. For large drive frequencies (Sr_p~1) all modes tend to diminish.

1 Introduction

A micro hot-wire, whose diameter is about 10 microns, used in air flow measurements, experiences a low Reynolds (Re) local flow. Especially in turbulent flow measurements, hot-wires are subject to a flow containing a spectra of fluctuations about a mean flow. Such flows can be represented by a low Re local mean flow and a steady-periodic fluctuating flow consisting of three dimensional waves traveling with a range of phase velocities and frequencies. Heat transfer in oscillatory flows at high frequencies with low mean flow Reynolds numbers is not well studied. In this work, we report a numerical study of low Re mean flow accompanied by a single fluctuating wave. These results are applicable to hot-wire measurements, where accurate heat transfer measurements are extremely important for calibration of the voltage output with respect to measurement of periodic fluctuations present in a turbulent or transitional flow.

Low Reynolds number flows over a stationary cylinder are well-studied. Batchelor (2000) gives a very good description of this flow and its regimes. In summary, Stokes flow is valid for up to Re = 0.25, for which one can hardly distinguish the fore-and-aft symmetry in the flow; for about Re = 10 a recirculation zone behind the cylinder is clearly visible; between Re = 30 and 40, first signs of instability are observed somewhat away from the cylinder in downstream, and as Re increases this instability moves closer to the cylinder; for about Re = 60, two standing eddies form immediately behind the cylinder on each side; these two eddies are the well-known Karman vortex streets and as Re increases further they are very much deformed immediately behind the cylinder but continues to form and move apart in downstream wake [Batchelor (2000)]. Experimental results of Williamson (1988, 1989) and numerical results of Sheard *et al* (2003) identified the onset of instability (break up of steady recirculation zone, and formation of wakes behind the cylinder) occurring at Re = 49 and 47 respectively.

Interaction between two-dimensional oscillatory flows and wakes of circular cylinders are studied by several authors such as Maull and Milliner (1978) and Laake and Eckelmann (1989); similarly a group of authors studied vortex formation in flow around an oscillating cylinder such as Sarpkaya (1979), Hall (1984), and Dutsch *et al* (1998). Two group of work report similar effects on the drag and lift coefficients. Despite the relative strength of interest in the flow and vortex structures, heat transfer from a cylinder in a low Re oscillatory flow or from an oscillating cylinder has not received as much attention. Fu and Tong (2002) investigated heat transfer from a heated oscillating cylinder in air cross flow. They implemented an Arbitrary Lagrangian-Eulerian (ALE) kinematic description to consider the moving interface between the fluid and the cylinder. They observed that, for Re = 200, the resonance mechanism in the lock-in regime helps augmenting the heat transfer from the cylinder. A thorough analysis of the laminar convective heat transfer from a cylinder in low frequency zero-mean oscillating flow is reported by Iwai *et al* (2004). They concluded that heat transfer is enhanced due to local fluid motion induced by the vortices around the cylinder. However, in the absence of mean flow, local warming effect somewhat diminishes the heat transfer enhancement (Iwai *et al* (2004)).

A body of work is related to acoustic enhancement of the heat transfer between heated surfaces and compressible flows. Gopinath and Harder (2000) report an experimental study of heat transfer from a cylinder in low-amplitude zero-mean oscillatory flow. Authors identify two distinct flow regimes: (1) laminar flow regime with a square-root dependence of the Nusselt number on the streaming Reynolds number based on the velocity amplitude of the wave; and (2) an unstable regime where vortex shedding from the cylinder leads to enhanced heat transfer rates. Komarov and Hirasawa (2003) report enhancement of heat transfer from a heated wire by application of an acoustic field in the gas flow. Authors conclude that heat transfer coefficient increases with the strength of the sound waves, and the Nusselt number is proportional to the square root of the Reynolds number based on the amplitude of gas velocity in the sound wave. Heat transfer enhancement due to acoustic effect diminishes as the wire temperature increases due to radiation and the strength of local free convection (Komarov and Hirasawa (2003)).

In this work, we report heat transfer results for near critical (Re = 50) and subcritical (Re = 10 and 30) mean flows over a cylinder accompanied by a single oscillatory periodic component. In section 2, our method and its numerical implementation are described, in 3 our results are reported and a summary of results and conclusion are presented in section 4.

2 Modeling Approach

2.1 Governing equations

Consider a two-dimensional flow over a cylindrical microwire shown in Figure 1. Due to small size of the wire (tens of micrometers), local flow in the vicinity of the wire can be considered as two-dimensional and laminar, and described as the sum of mean, $\mathbf{u}_0$, and periodic flows, $\mathbf{u}_\mathrm{p}$, as follows:

$$\mathbf{u}(\mathbf{x},t) = \mathbf{u}_0(\mathbf{x},t) + \mathbf{u}_\mathbf{p}(\mathbf{x},t). \tag{1}$$

The periodic flow, in general, may contain a number of traveling-waves in the x-direction, and time-periodic oscillations in the y-direction, for example:

$$\mathbf{u}_\mathbf{p}(\mathbf{x},t) = \sum_{j=1}^{N} \left[u_j \sin\left(\omega_j t - k_j x\right) \quad v_j \sin\left(\omega_j t\right) \right]', \tag{2}$$

where u_j is the amplitude of the j^{th} traveling wave in the x-direction, ω_j is its angular frequency, k_j is the wave-number equal to $1/\lambda_j$, $\lambda_j = c/\omega_j$ is the wavelength in the x-direction, c is the phase velocity, and v_j is the amplitude of the cross-flow oscillations the y-direction.

Flow field given by (1) is governed by continuity and Navier-Stokes equations as follows:

$$\nabla \cdot \mathbf{u}_0(\mathbf{x},t) = -\nabla \cdot \mathbf{u}_\mathbf{p}(\mathbf{x},t); \tag{3}$$

and

$$\rho \frac{\mathrm{d}\mathbf{u}_0}{\mathrm{d}t} = -\nabla p + \mu \nabla^2 \mathbf{u}_0 + \left(\mu \nabla^2 \mathbf{u}_\mathbf{p} - \rho \frac{\mathrm{d}\mathbf{u}_\mathbf{p}(\mathbf{x},t)}{\mathrm{d}t} \right), \tag{4}$$

where ρ is density, p is pressure, and μ is viscosity of the fluid. When the flow has only time-periodic waves but not the traveling-waves, right-hand-side of the continuity equation in (3) for the mean flow becomes zero, however, Navier-Stokes equation for the mean flow, $\mathbf{u}_0$, always contains an artificial body force due to periodic; see the last term on the right-hand-side of (4). This body force is identified as an artificial pressure-gradient in a similar approach used by Iwai *et al* (2004).

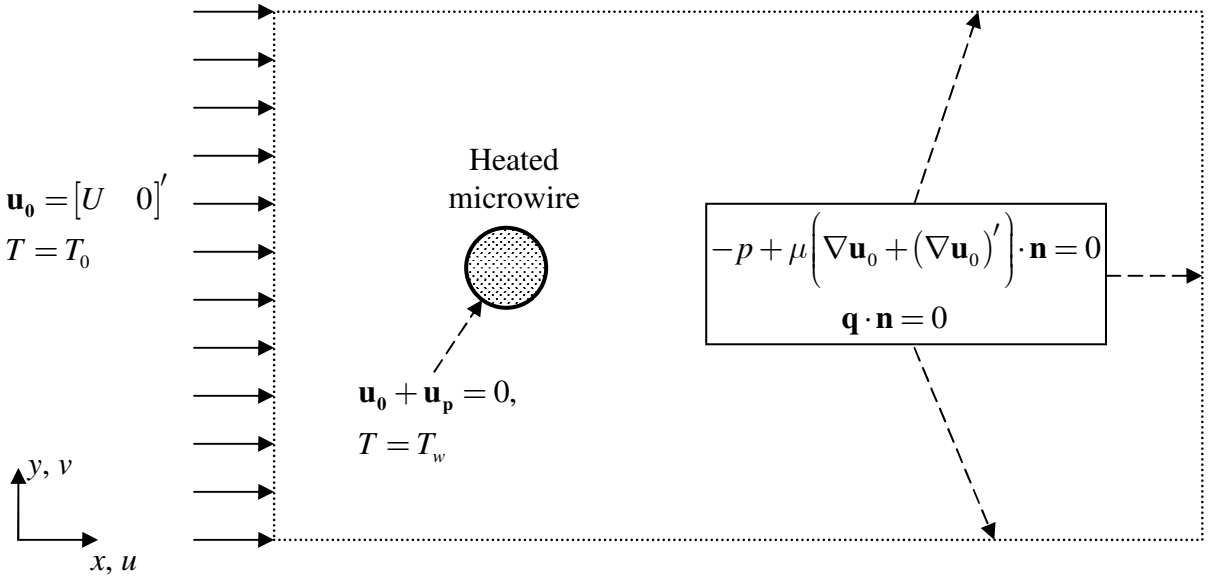

Figure 1. A sketch of local two-dimensional flow over a heated microwire, and respective bondary conditions for velocity and temperature.

In the special case, where the local two-dimensional flow across the wire contains only fluctuations in the *y*-direction, that is

$$\mathbf{u}_\mathbf{p}(\mathbf{x},t) = \left[0 \quad v_p \sin(\omega t) \right]', \tag{5}$$

the mean flow satisfies the continuity equation:

$$\nabla \cdot \mathbf{u}_0(\mathbf{x},t) = 0. \tag{6}$$

For this case, the momentum equation becomes:

$$\rho \frac{\mathrm{d}\mathbf{u}_0}{\mathrm{d}t} = -\nabla p + \mu \nabla^2 \mathbf{u}_0 - \rho v_p \left[\sin(\omega t) \frac{\partial u}{\partial y} \quad \omega \cos(\omega t) + \sin(\omega t) \frac{\partial v}{\partial y} \right]'. \tag{7}$$

Boundary conditions for equation (7) are presented in Figure 1, where a finite region around the wire is implemented to truncate the space around the wire. Upstream average velocity of the mean flow is specified, $\mathbf{u_0} = U$, sufficiently away from the wire such that temperature gradient on that boundary is almost zero. Due to no-slip boundary conditions for total flow on the wire surface, mean flow is set to negative of the periodic flow on the wire. Rest of the boundaries corresponding to outflow conditions are specified as zero net normal stress so as to impose a condition of neutrality for flow (Figure 1).

Governing equation of the temperature distribution within the fluid is the standard convection equation given by:

$$\rho c_p \left(\frac{\partial T}{\partial t} + \mathbf{u} \cdot \nabla T \right) = k \nabla^2 T \,, \tag{8}$$

where the velocity **u** is given by (1) as the sum of the mean, $\mathbf{u}_0$, and the periodic, $\mathbf{u}_p$, components, c_p is the specific heat, and k thermal conductivity of the fluid. Convection equation, (8), is subject to boundary conditions specified in Figure 1: upstream fluid is at constant temperature, T_0, wire surface is at T_w, and the rest of the boundaries are specified as neutral convective flux, which corresponds to zero heat flux in the normal direction. Initially flow is at steady-state without the periodic component, and at constant temperature T_0.

2.2 Numerical approach

For the properties and geometric dimensions specified in Table 1, a commercial finite-element solver Comsol Multiphysics 3.2 is used for solution of the nondimensional form of equations (7) and (8). Triangular elements, quadratic for velocity and temperature and linear for pressure, are used for the discretization of the computational domain. Two different computational domains are used, one for Re = 10, and one for Re = 30 and 50, which contain about 50,000 and 42,000 degrees of freedom respectively. Computational domain for Re = 10 has a longer upstream section before the cylinder due to relative importance of conduction for low Re.

Simulations are carried out starting from initial steady-state conditions for all forced frequencies of the periodic component of the v-velocity. Nondimensional frequency of the forced-input wave is given by a group akin to Strouhal number of the natural vortex shedding from the cylinder:

$$Sr_p = \frac{\omega D}{2\pi U}, \tag{9}$$

where, D is microwire's diameter, U is the upstream mean-flow velocity in the x-direction, and ω is the angular frequency of the forced input-wave.

To obtain the heat transfer response to fluctuating flow, we use Nusselt numbers at the stagnation point, and averaged over the surface of the cylinder. Simulations are carried out for a reasonably long duration (150 time units followed by 2 full periods) to obtain the heat transfer response. A version of the Fast Fourier Transfer (FFT) algorithm of MATLAB is used to calculate the response amplitudes for each mode. This is especially necessary for Re = 30 and 50, as the response contains the natural vortex shedding frequencies and its harmonics as well.

Table 1. Properties and dimensions used in simulations

Air properties at 300 K	
Density, ρ (kg/m^3)	1.177
Specific heat, c_p (J/kg-K)	1005
Thermal conductivity, k (W/m-K)	.0267
Viscosity, μ (kg/m-s)	.184 x 10^{-4}
Wire's Dimensions	
Diameter	10 μm

3 Results and Discussion

Amplitude response of the stagnation and average Nusselt numbers, as well as their time-averaged values are calculated from simulations carried out for each driving frequency. Time-averaged values are obtained from averaging out of the time signal as follows:

$$\langle Nu_a \rangle = \left(\frac{D}{\Delta T}\right)\frac{1}{K\Delta t}\sum_{k=0}^{K}\left[\int_{cyl}\frac{dT}{d\mathbf{n}}ds\right]_{t_k}, \tag{10}$$

and

$$\langle Nu_s \rangle = \left(\frac{D}{\Delta T}\right)\frac{1}{K\Delta t}\sum_{k=0}^{K}\left.\frac{dT}{d\mathbf{n}}\right|_{\theta=0,t=t_k} \tag{11}$$

In all cases, first 100 time units, where one unit is equal to nondimensional time, $\tau = D/U$, are used to ramp up the amplitude of oscillations from 0 to its full value to avoid numerical instabilities initially. For Re = 10 and 30, simulations start from the steady-state solution, for Re = 50, initial condition is the naturally vortex shedding steady-periodic flow without forced oscillations. Due to onset of the instability, the flow is already steady-periodic for Re = 50 even without the forced oscillations imposed on the flow. Strouhal number of the instability is Reynolds dependent, and is about *Sr* = 0.13 at the onset for Re = 47. The instability is due to a Hopf bifurcation, and in the subcritical region *Sr* drops rapidly as Re decreases according to Sheard *et al* (2003).

In Figure 2, variation of the time-averaged average Nusselt number over the cylinder with respect to forced *y*-oscillations of amplitude 0.1 and 0.2 (10% and 20% of the mean flow) is shown for Reynolds numbers 10, 30 and 50. In all three cases $<Nu_a>$ is normalized with respect to its base value, Nu_{a0}, which corresponds to the steady-state average Nusselt number for Re = 10 and 30, and time-averaged Nu_a in the case of Re = 50 due to its oscillatory nature. It is clear that as the Re increases, albeit small, Nu_a increases as well for V_p = 0.1. For Re = 50, increasing the amplitude of the *y*-oscillation does not improve average and stagnation Nusselt numbers. The improvement in $<Nu_a>$ is confined to a region near the onset of Strouhal instability. $<Nu_a>$ reaches its peak at Sr_p = *0.14*, *0.11*, and *0.03* for Re = 50, 30 and 10 respectively. According to data extracted from Sheard *et al* (2003), subcritical Strouhal numbers for Re = 10 and 30 are *Sr* = *0.07* and *0.10* are respectively. In Figure 3, a similar behavior for the stagnation Nusselt number is observed with smaller increase than the one for average Nusselt number. Maximum increases in $<Nu_s>$ are observed for Sr_p = *0.13*, *0.11*, and *0.03* for Re = 50, 30 and 10 respectively.

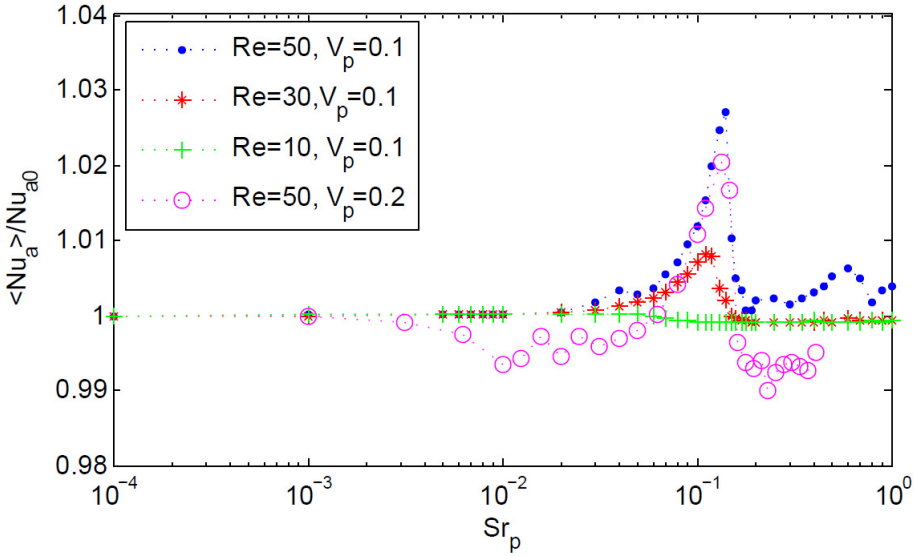

Figure 2: Variation of the time-averaged average Nusselt number with respect to frequency of forced oscillations for Re = 10,30 and 50, and V_p = 0.1 and 0.2.

Distribution of the amplitude of Nusselt number's response to forced oscillations is computed using the Fourier transform (FT) of the time response with the FFT implementation in MATLAB. This is necessary to compute response amplitudes of each mode separately. We must note that, despite its relatively easy use for the task, FT is not completely reliable when the time-signal is not periodic

with respect to all the components in the flow. We pay special attention to identify slower and faster components using two different output signals one lasting 200 time units with intervals of 1, and the other lasting 2 time periods of the drive sinusoidal with intervals of 40^{th} of each period.

Heat transfer from the heated cylinder reaches to maximum when the speed of flow (regardless of the direction) reaches to its maximum and to minimum when the speed is the smallest. This is generally true for oscillations with small driving frequencies prior to 'lock-in' type of effect in the flow. Hence, amplitude of the Nusselt number is usually the largest at the second harmonic of the driving frequency, i.e. $2 \times Sr_p$ for low Sr_p.

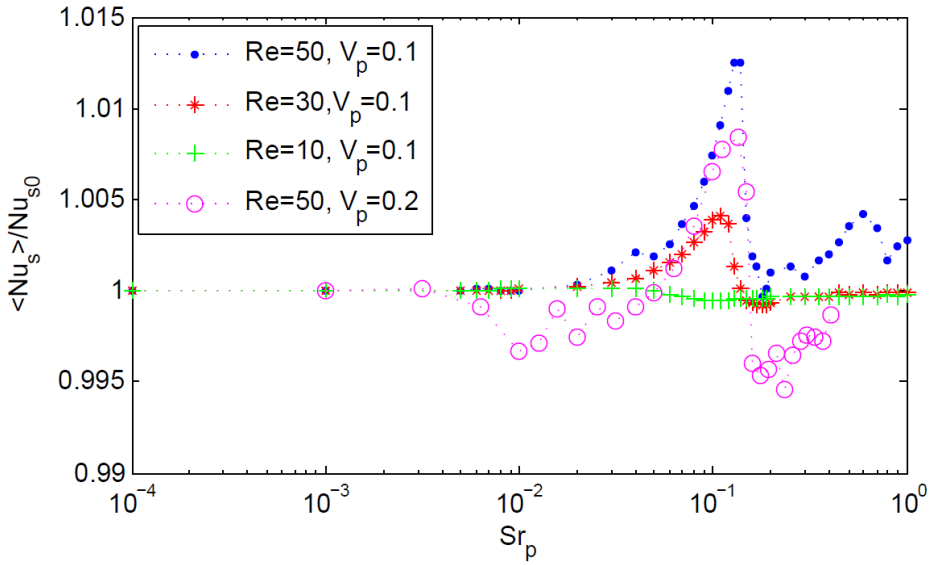

Figure 3: Variation of the time-averaged stagnation Nusselt number with respect to frequency of forced oscillations for Re = 10,30 and 50, and V_p = 0.1 and 0.2.

In Figures 4 to 6, the first mode refers to the responses of Nu_s and Nu_a (top and bottom graphs respectively) at the drive frequency, Sr_p., and the second mode to its 2^{nd} harmonic, $2 \times Sr_p$. For Re = 10 (Figure 4), first mode remains very small, and almost constant throughout the range of forced flow oscillations. However the second mode, whose frequency is equal to two times the frequency of the forced oscillations, is dominant for low frequencies. This is a typical behavior observed by Iwai *et al* (2004) for Nu, and Sarpkaya (1979) for the drag coefficient. Regardless of the direction of the *v*-oscillation in the flow, heat transfer is augmented due to sheer increase of the flow speed. Amplitude of the second mode remains almost constant up to frequencies in the resonant region. When Sr_p gets closer to subcritical *Sr* values, the second mode of the Nu gets damped. Second mode's response is classic first order response, with a cut-off frequency near the frequency of the instability. We think that the rise of the amplitude response of the second mode towards Sr_p = 1, is purely numerical as it shows erratic behavior in small amplitudes and small time-windows used for the FFT algorithm.

In Figure 5, as in the case for Re = 10, for low $Sr_p < 0.01$, stagnation and average *Nu* amplitudes remain unchanged compared to the case without *v*-fluctuations in the flow. The second mode of the *Nu* oscillations for which the frequency of the response is twice the frequency of the forced periodic flow is dominant for up to $Sr_p \approx 0.01$. However, unlike for Re = 10, the emergence of the first mode for $Sr_p > 0.1$ is more prominent. The first mode, for which the *Nu* oscillations have the same frequency as the forced oscillations of the flow, first increases to its highest value, which is as much as the highest value of the second mode for Nu_s, then declines. Unlike the second mode, first mode

shows a higher order response characteristic especially for the stagnation Nusselt number as shown in top graph in Figure 5. Both first and second modes decline rapidly for higher values of Sr_p; somewhat increase of the second mode for $Sr_p \rightarrow 1$ is likely to be a numerical artifact as in the case for Re = 10. Despite our efforts to single out this case with longer simulations, we are not convinced that the rise of the second mode is systematic. Further detailed and more accurate simulations are necessary to identify the behavior for that range of drive frequencies.

In Figure 6, responses of Nu_s and Nu_a are shown for Re = 50. Due to inherent presence of the vortices in the flow, decomposition of the response into its components is more error prone here than for Re = 10 and 30. Some of the choppiness especially for low amplitudes may be due to inaccuracies in the calculation of modal amplitudes. However, it is obvious that similar to the cases for Re = 10 and 30, the second mode is more prominent for up to Sr_p = .1 especially for Nu_s. In fact, here, first mode amplitude increases above the second mode amplitude for Sr_p > .1. However, for Nu_a, a clear dominance of the first mode amplitude over the second mode is not obvious.

In Figure 7, a comparison of the second mode amplitudes for Re = 10, 30 and 50 is shown. Clearly, as Reynolds number of the mean flow increases, amplitude of the stagnation Nusselt's second mode increases for fixed drive amplitude of 0.1 for all cases. Despite a smooth decline for Re = 10, amplitude of the 2nd mode declines sharply for Re = 30 and 50 for $Sr_p > 0.1$, and is even accompanied by a small increase for Re = 50 where it reaches to its maximum at $Sr_p = 0.13$. A slight increase in the 2nd-mode amplitude is also observed for Re = 30, where its exact maximum is observed at $Sr_p = 0.04$, and where the increase is smooth within a range of $0.04 < Sr_p < 0.11$.

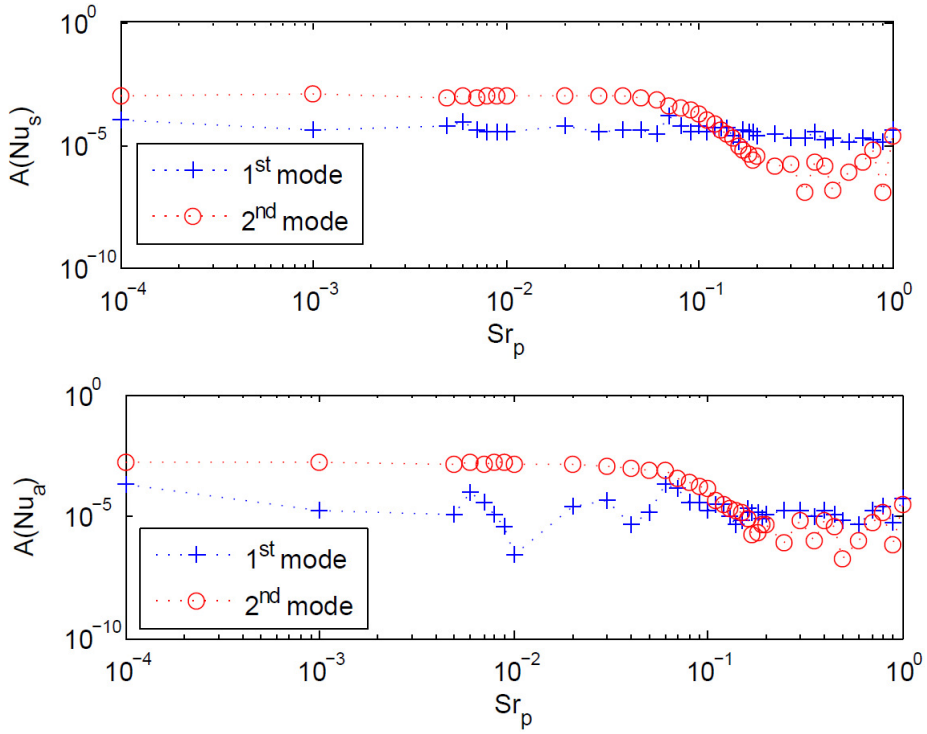

Figure 4. Amplitude of the first two modes of stagnation Nusselt number response for Re = 10, where the first mode is the same frequency as the driving oscillations, and the second mode's frequency is the twice as much the frequency of the driving oscillations. *Top*: Stagnation Nusselt number; *Bottom*: Average Nusselt number.

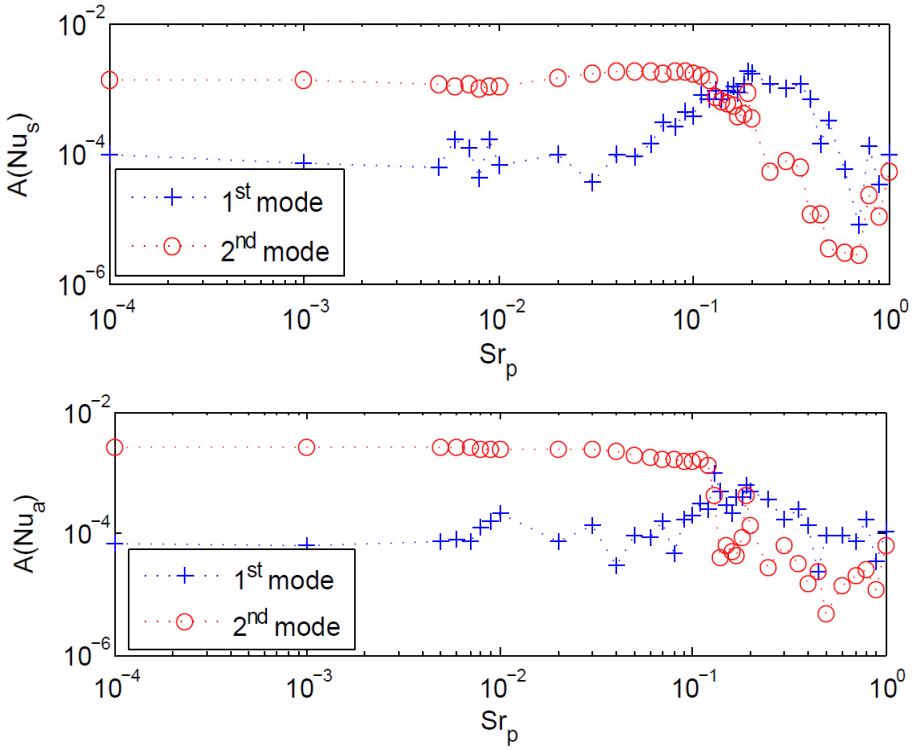

Figure 5: Amplitude of the first two modes of stagnation Nusselt number response for Re = 30, where the first mode is the same frequency as the driving oscillations, and the second mode's frequency is the twice as much the frequency of the driving oscillations. *Top*: Stagnation Nusselt number; *Bottom*: Average Nusselt number.

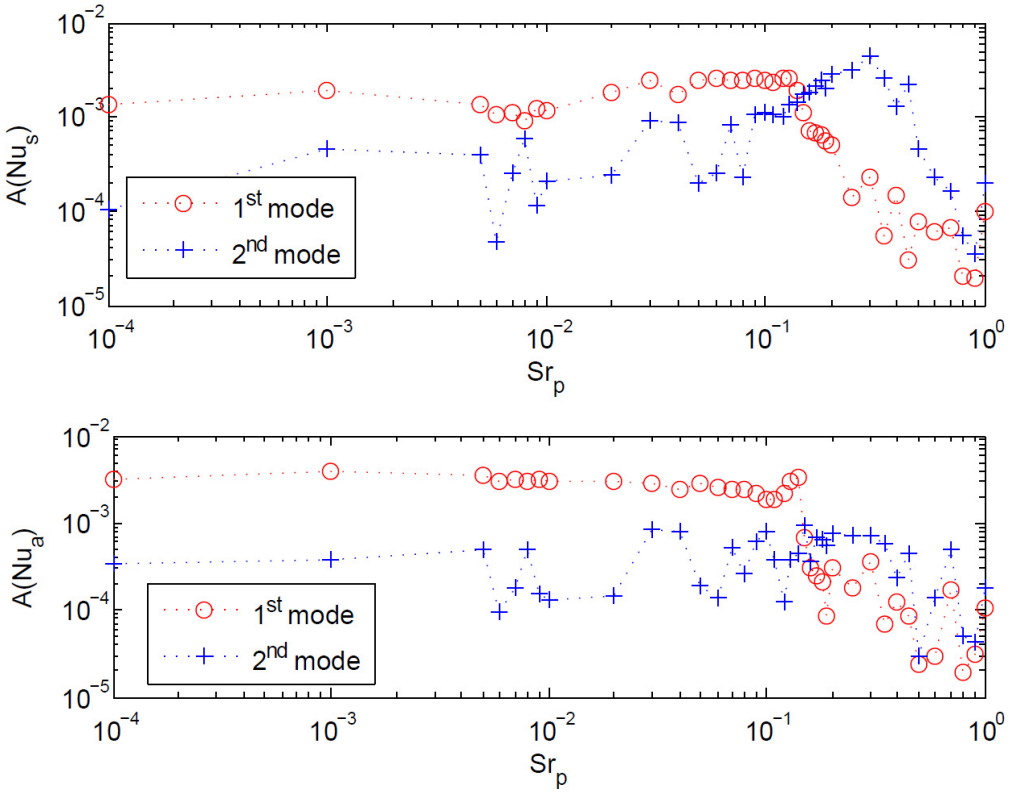

Figure 6: Amplitude of the first two modes of stagnation Nusselt number response for Re = 50, where the first mode is the same frequency as the driving oscillations and the second mode's frequency is the twice as much the frequency of the driving oscillations. *Top*: Stagnation Nusselt number; *Bottom*: Average Nusselt number.

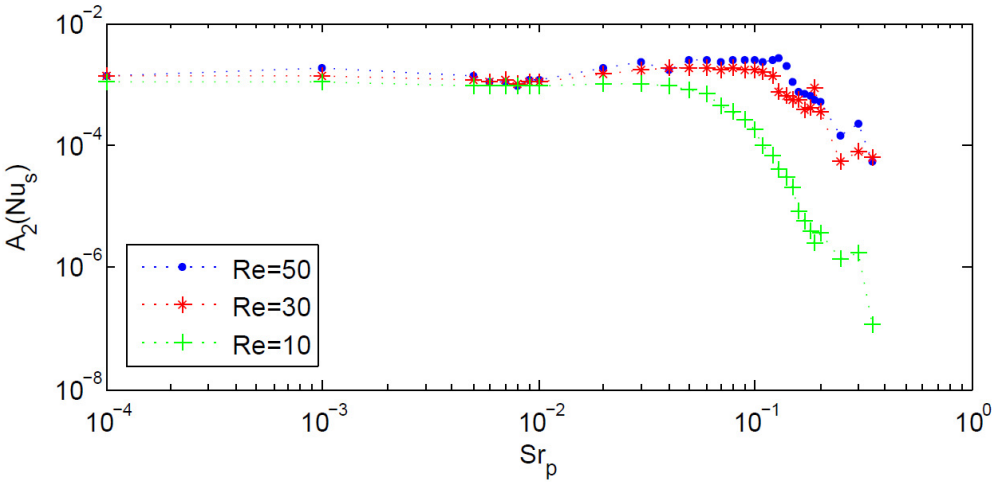

Figure 7: Comparison of the second mode amplitudes of stagnation Nusselt number for Re = 10, 30 and 50 for *v*-oscillations of amplitude 0.1 (10% of the mean flow).

4 Conclusion

Using finite-element simulations, we carried out an extensive study for the effect of the *y*-oscillations in the flow on the heat transfer from a heated wire for sub- and near critical mean flows of Re = 10, 30 and 50. We solved for the time-dependent mean flow by adding an artificial body force (or pressure gradient) resulting from the time derivative and inertial effects of the periodic component of the flow. Our method proved to be viable and stable for the range of Reynolds number and drive frequencies of our interest. Our results indicate that one cannot conclude easily if there is a strong effect of the oscillations on the time-averaged stagnation and Nusselt numbers. We have observed very small variations in the average Nusselt numbers. The maximum increase in Nusselt number, about 3%, is observed for Re = 50 (for which the flow is already steady-periodic without forced oscillations) and for oscillation amplitude of V_p = 0.1 in nondimensional quantities (corresponding to 10% of the magnitude of the mean flow). Further increase in the oscillation amplitude does not yield an increase in the Nusselt number, in fact, even a slight decrease is observed. Maxima of the average Nusselt numbers are observed at frequencies that agree with the subcritical Strouhal numbers.

Amplitude of the oscillations of the Nusselt number shows a multimodal character. We have used Fourier Transform to identify amplitudes of each mode. According to our results, heat transfer oscillations are dominated, first, at frequencies twice as much as the drive frequency for small driving frequencies; then as the drive frequency is increased a type of lock-in phenomenon results in Nusselt oscillations at the drive frequency.

Further simulation results are necessary to identify all the response frequencies of the heat transfer and their amplitudes especially for $Sr_p>0.1$.

REFERENCES

Batchelor, G.K., 2000, *Introduction to fluid dynamics*, Cambridge University Press.

Dutsch, H., Durst,F., Becker, S. and Lienhart, H., 1998, 'Low-Reynolds-number flow around and oscillating circular cylinder at low Keulegan-Carpenter numbers', *J Fluid Mech*, 360, 249-271.

Gopinath, A., and Harder, D., 2000, 'An experimental study of heat transfer from a cylinder in low-amplitude zero-mean oscillatory flows', *Int J of Heat and Mass Trans*, 43, 505-520.

Hall, P., 1984, 'On the stability of the unsteady boundary layer on a cylinder oscillating tranversely in a viscous fluid', *J Fluid Mech*, 146, 347-367.

Iwai, H., Mambo, T., Yamamoto, N., and Suzuki, K., 2004, 'Laminar convective heat transfer from a circular cylinder exposed to a low frequency zero-mean velocity oscillating flow', *Int J of Heat and Mass Trans*, 47, 4659-4672.

Komarov, S. and Hirasawa, M., 2003, 'Enhancement of gas phase heat transfer by acoustic field application', *Ultrasonics*, 41, 289-293.

Laake, E.D. and Eckelmann, H. 1989, 'Phenomenology of Karman vortex streets in oscillatory flow', *Experiments in Fluids*, 7, 2, 217-227.

Maull, D.J. and Milliner, M.G., 1978, 'Sinusoidal flow past a circular cylinder, Coastal Engineering', 2, 149-168.

Sarpkaya, T., 1979, 'Vortex-induced oscillations: A selective review', 46, 241-258.

Sheard, G.J., Thompson, M.C., and Hourigan, K., 2003, 'From spheres to circular cylinders: the stability and flow structures of bluff ring wakes', *J Fluid Mech*, 492, 147-180.

Williamson, C., 1988, 'Defining a universal and continuous Strouhal–Reynolds number relationship for the laminar vortex shedding of a circular cylinder', *Phys. Fluids*, 31, 2742–2744.

Williamson, C., 1989, 'Oblique and parallel mode of vortex shedding in the wake of a circular cylinder at low Reynolds numbers', *J Fluid Mech*, 206, 579–627.